

Supplementary information

Direction-oriented fiber guiding with tunable tri-layer-3D scaffold for periodontal regeneration

Sarin Abraham,^a Pallavi Gupta,^a Kavitha Govarthanan,^b Suresh Rao,^a and Tuhin Subhra Santra^{*a}

a. Department of Engineering Design, Indian Institute of Technology Madras, Chennai- 600036, India.

b. Institute for Stem Cell Science and Regenerative Medicine (DBT-inStem), Bengaluru, Karnataka - 560065, India

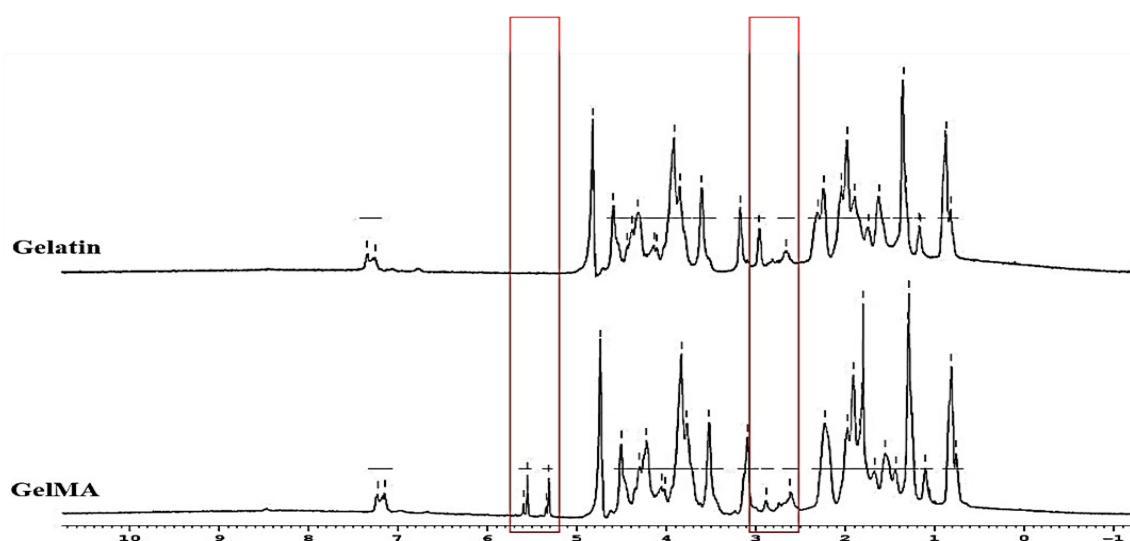


Figure S1. Characterization of GelMA using ¹H NMR spectra of Gelatin and GelMA

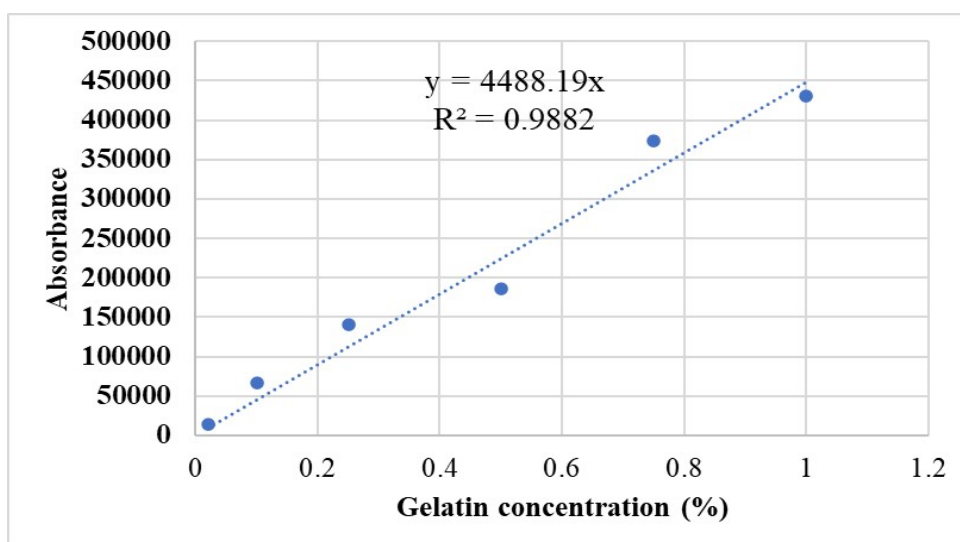


Figure S2. Calibration plot for Fluoraldehyde assay for DoF calculation

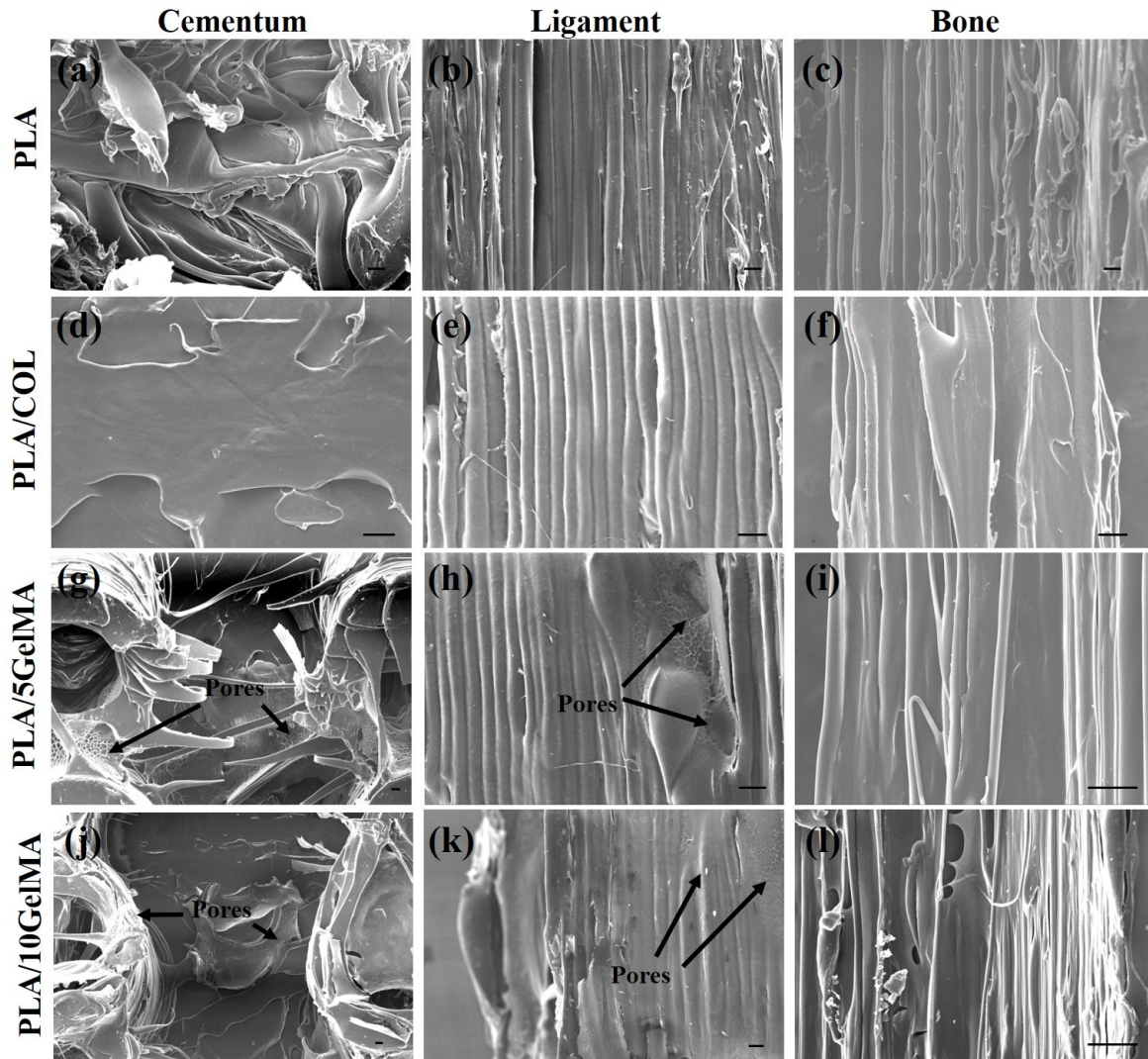


Figure S3: The Scanning Electron Microscopy (SEM) images of cementum, periodontal ligament and bone layer. (a,b,c) shows the intricate micro topology of control PLA scaffold with cementum, ligament and bone layers. (d,e,f) illustrate the relatively smoother topology of PLA/COL scaffolds with cementum, ligament and bone layers. (g,h,i) indicate the surface of PLA/5GelMA surface with cementum, ligament and bone layers. The pores on the scaffold due to GelMA coating are clearly visible in (g) and (h). (j,k,l) shows the surface topography of PLA/10GelMA scaffold with cementum, ligament and bone layers. The decreased pore size is indicated in (j) and (k). Scale for all images is 100 μ m.

Group	Cementum scaffold Root mean square roughness (Rq) (nm)	Bone Scaffold Root mean square roughness (Rq) (nm)
PLA	109.3 \pm 15.8	77.27 \pm 16.23
PLA/COL	72.16 \pm 38.39	36.9 \pm 3.83
PLA/5GelMA	71.17 \pm 27.63	48.5 \pm 21.7
PLA/10GelMA	57.33 \pm 13.64	30.4 \pm 7.07

Table S1. Comparison root means square roughness of PLA, PLA/COL, PLA/5GelMA, and PLA/10GelMA scaffolds by AFM. All data are reported as mean \pm standard deviation (n = 3).

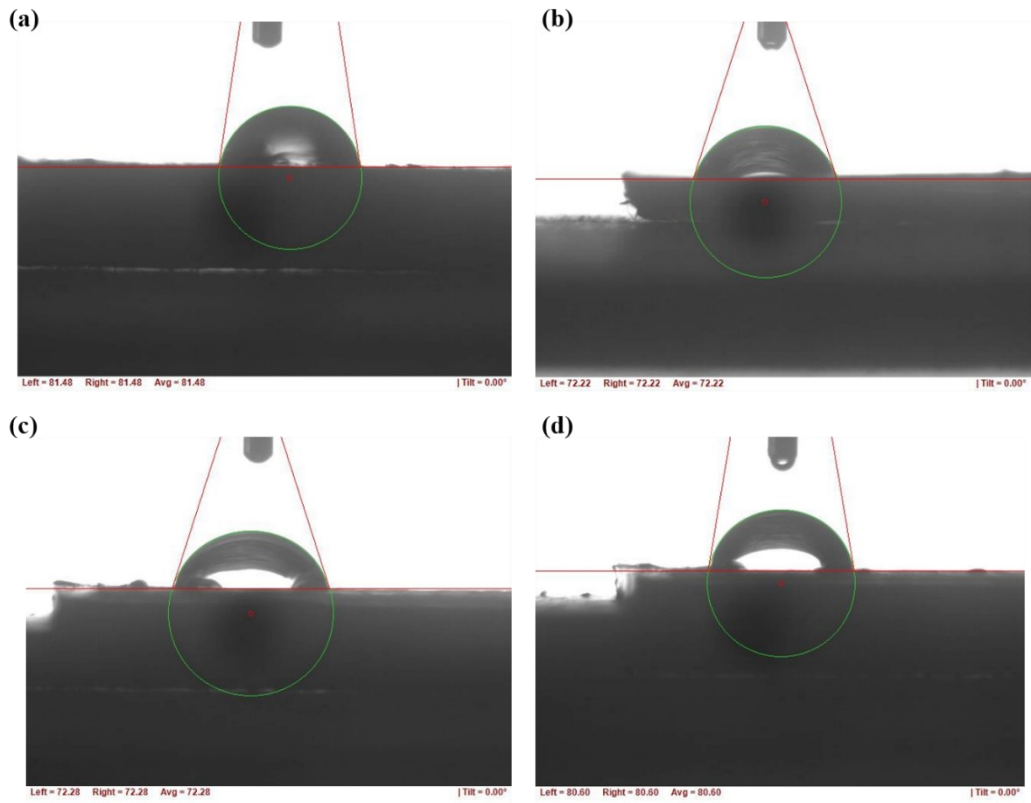


Figure S4. The contact angle of bone layer (a)PLA control scaffold, (b) PLA/COL scaffold, (c) PLA/5GelMA, and (d) PLA/10GelMA

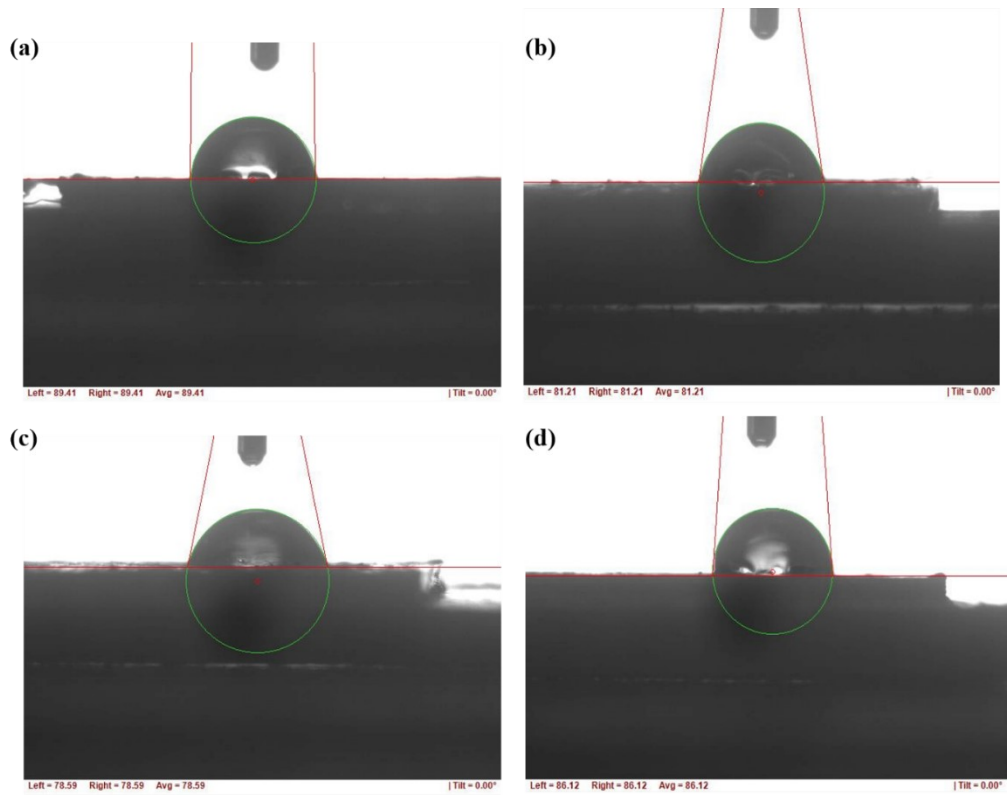


Fig S5: Contact angle of cementum layer (a)PLA scaffold, (b) PLA/COL scaffold, (c) PLA/5GelMA, and (d) PLA/10GelMA

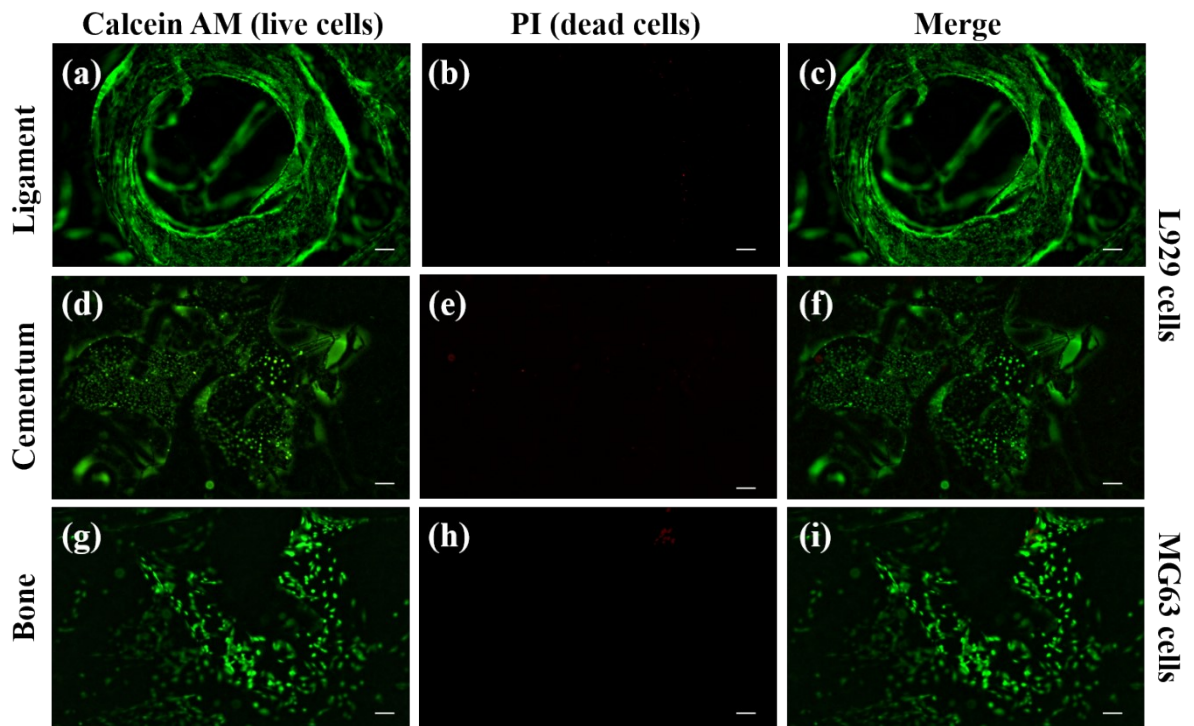


Figure S6. Cell culture on PLA/COL scaffold (a) Live L929 cell staining on ligament (b) dead L929 cells on ligament (c) merged image of (a) and (b), (d) Live L929 cell staining on cementum (b) dead L929 cells on cementum (c) merged image of (d) and (e), (g) Live MG63 cell staining on bone (h) dead MG63 cells on bone (i) merged image of (g) and (h). Calcein AM stain live(green) and PI dyes stain dead cells (red). Scale for all images is 200 μ m.

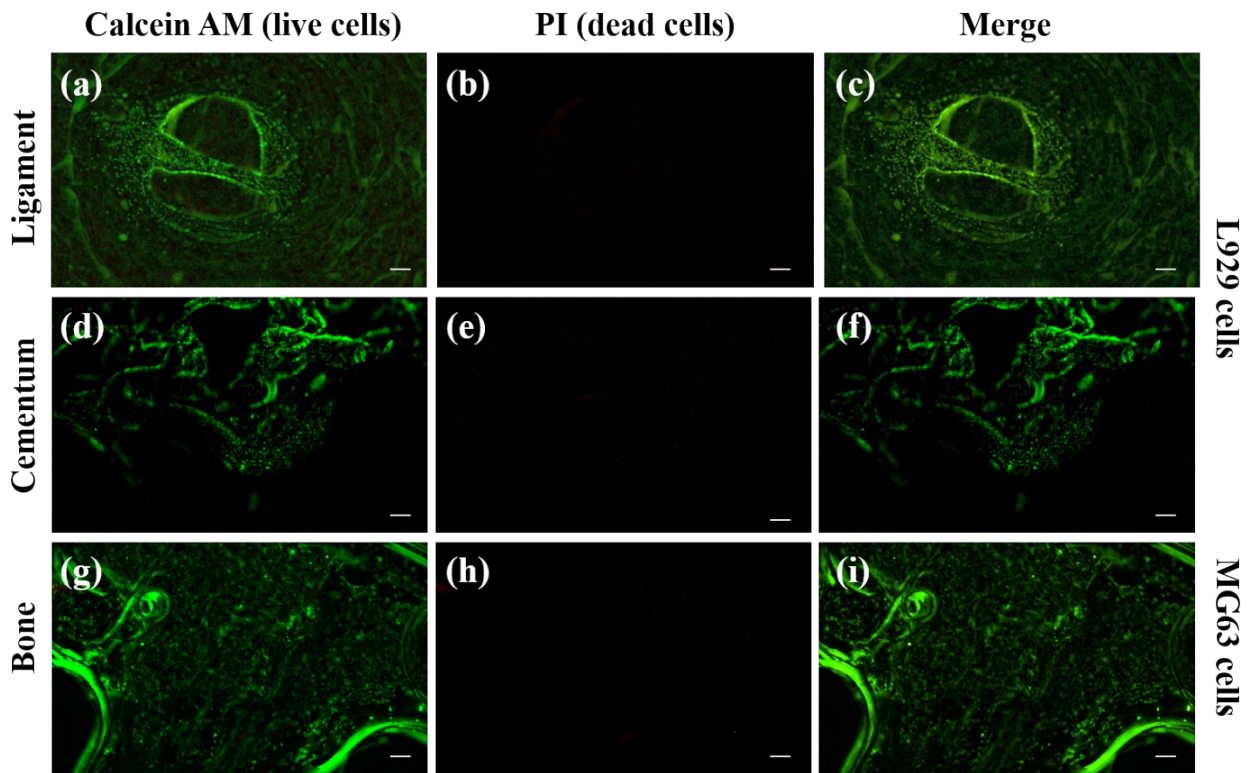


Figure S7. Cell culture on PLA/5GelMA scaffold (a) Live L929 cell staining on ligament (b) dead L929 cells on ligament (c) merged image of (a) and (b), (d) Live L929 cell staining on cementum (e) dead L929 cells on cementum (f) merged image of (d) and (e), (g) Live MG63 cell staining on bone (h) dead MG63 cells on bone (i) merged image of (g) and (h). Calcein AM stain live (green) and PI dyes stain dead cells (red). Scale for all images is 200 μ m.

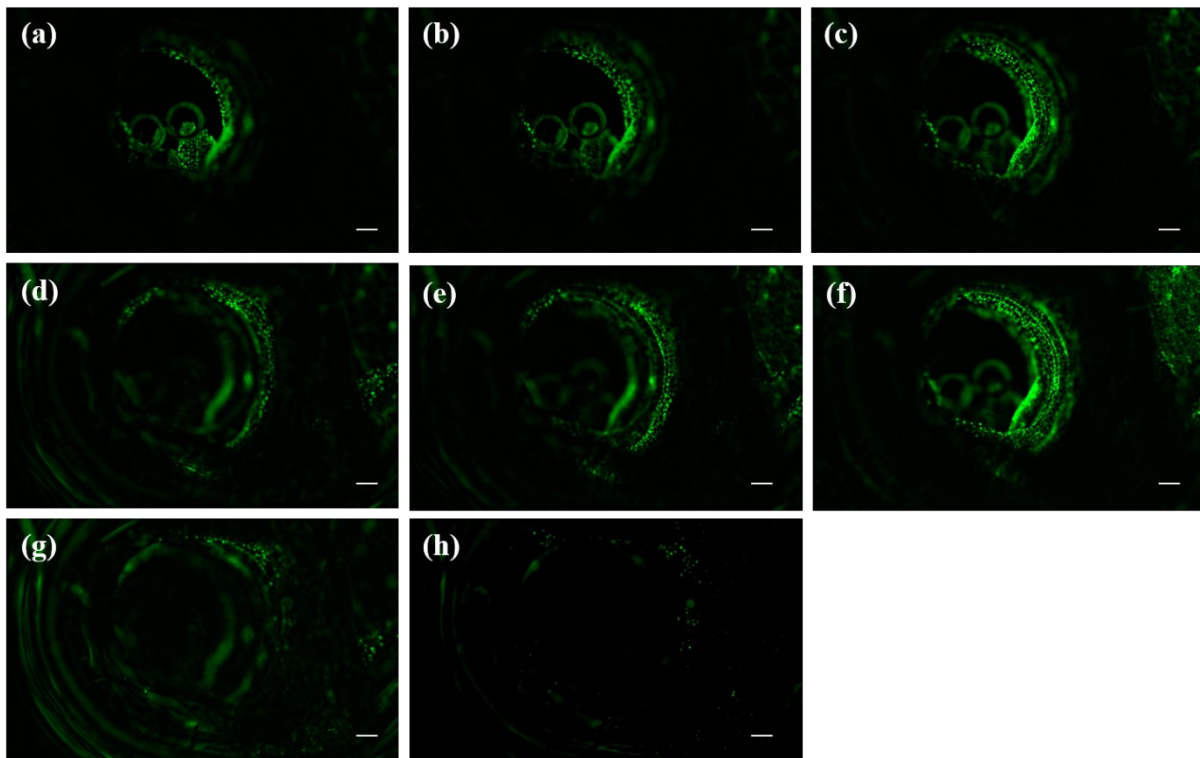


Figure S8. L929 cell inside the periodontal ligament on PLA/5GelMA scaffold. The images are taken at different depth inside the periodontal ligament. Scale for all images is 200 μ m.

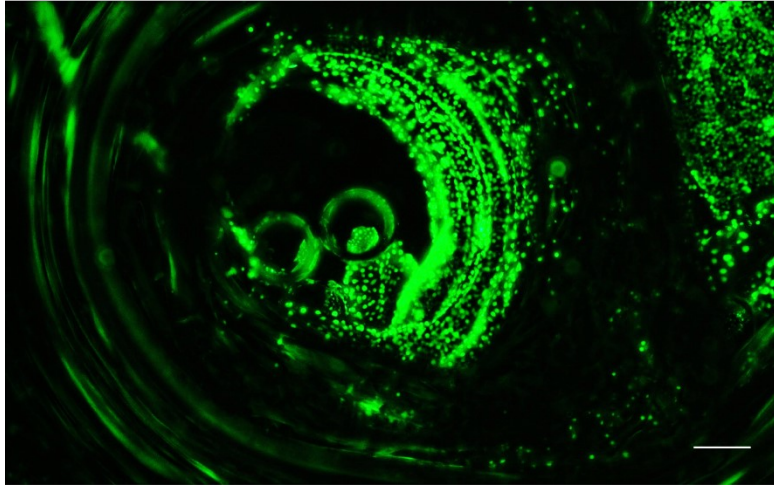


Figure S9. L929 cell inside the periodontal ligament on PLA/5GelMA scaffold. The images are taken at different depth inside the periodontal ligament are stacked to form the image. Scale for the image is 200 μ m.

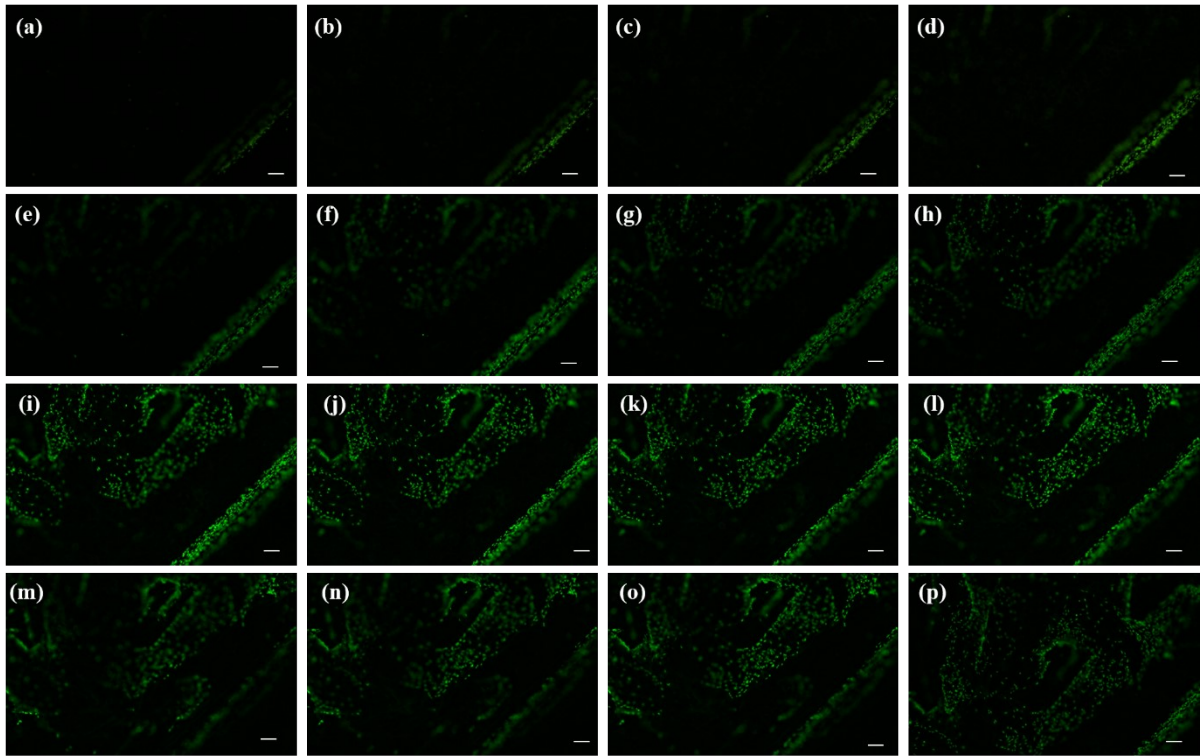


Figure S10. Live L929 cell on top of the cementum shelf on PLA scaffold. The images are taken at different depth on the cementum shelf and on the cementum surface. Scale for the image is 200 μ m.

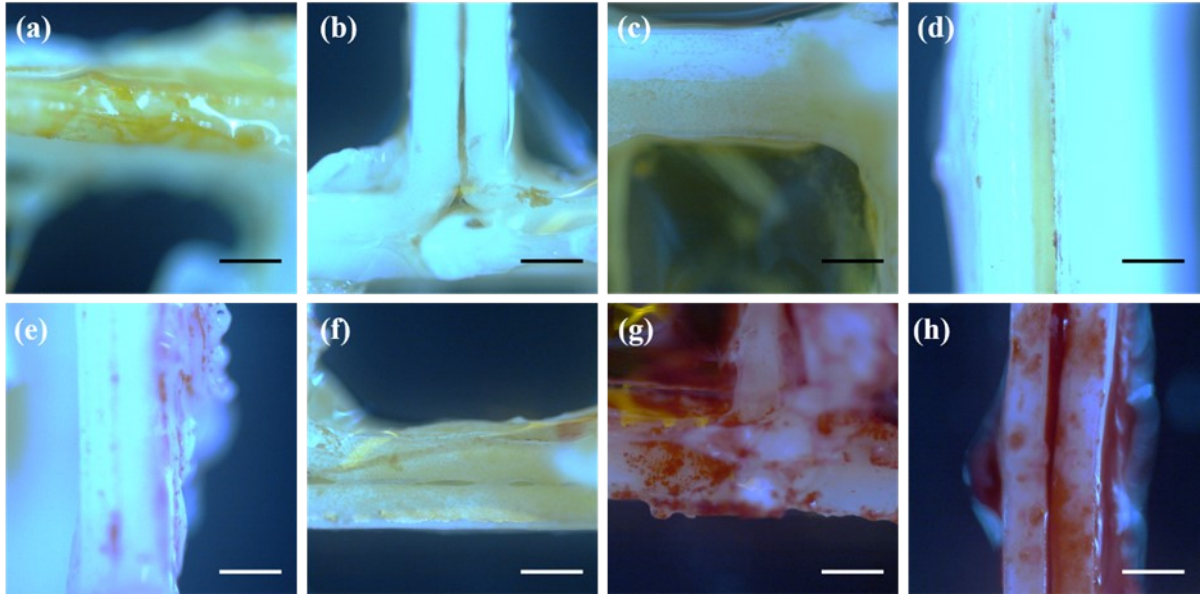


Figure S11: Alizarin red S staining of MG63 cells. Cells cultured in DMEM media on (a) PLA (b) PLA/COL, (c) PLA/5GelMA and (d) PLA/10GelMA bone layers. Cells cultured in osteogenic media on (e) PLA (f) PLA/COL, (g) PLA/5GelMA and (h) PLA/10GelMA bone layers. The MG63 cells were cultured on various specimens for 7 days. Scale for images 500 μ m.

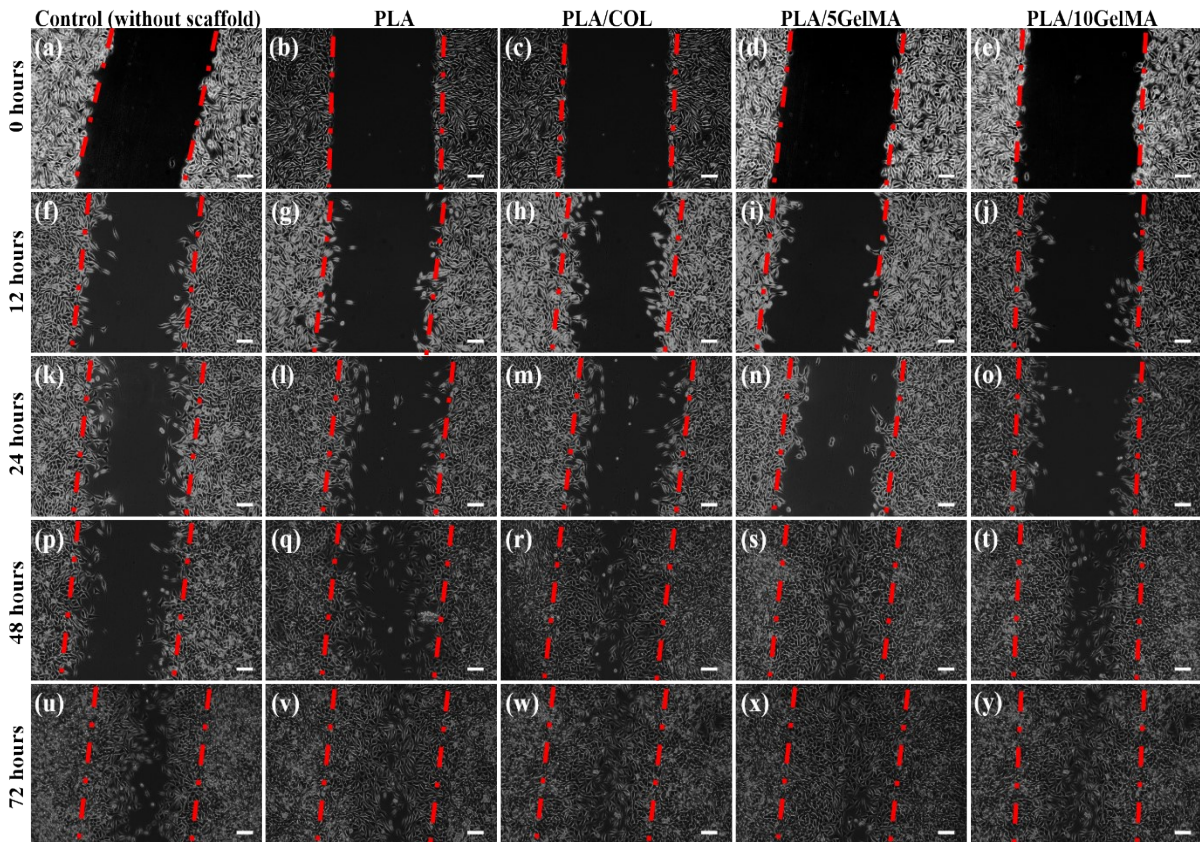


Figure S12: The effectiveness of the different scaffolds was measured by In vitro wound healing assay using L929 cells. Microscopic images showing the scratched area at the beginning of experiment (0 hours), 12 hours, 24 hours, 48 hours, and after 72 hours migration cell (scratch assay) using inverted

microscope (IX73, Olympus, Japan). Red dotted lines indicate initial scratch edges. Scale for the image is 200 μ m

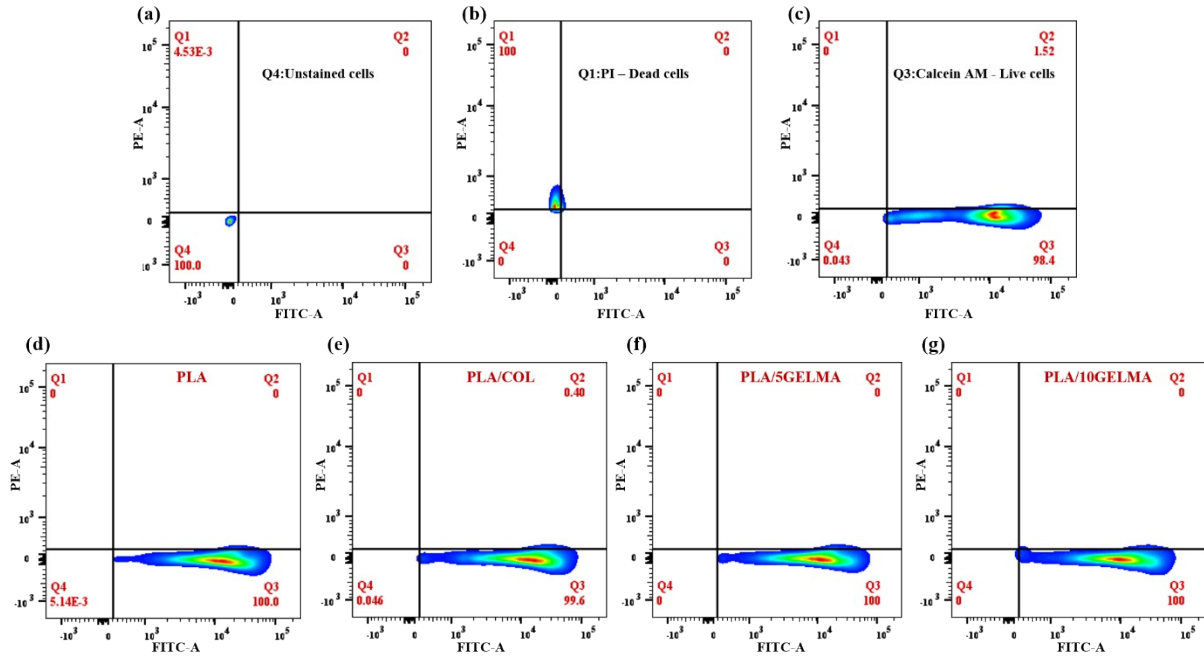


Figure S13. Flow cytometry-based quantification of live and dead MG63 cells on scaffolds. (a) unstained MG63 cell population (b) cell stained with PI dye (dead cells) (c) cells stained with calcein AM (live cells) (d) the percentage of live and dead cells on PLA scaffold (e) the percentage of live and dead cells on PLA/COL scaffold (f) the percentage of live and dead cells on 5GELMA scaffold (g) the percentage of live and dead cells on PLA/10GelMA scaffold after 1 day incubation.

	Compressive strength	Anchorage of the ligament to bone and cementum layers	Cell viability	Customizable scaffold	Multiple oriented fibers	Technology used	Material used	Regenerative layers
Our proposed work	13.48MPa to 14.36MPa	Yes	100% for L929 and MG63 cell lines (from flow cytometry results)	Yes	Yes	FDM	PLA with collagen and (GelMA) coating	Yes
Sowmya et al¹	Not mentioned	No	Good	No	No	Solution was frozen, and lyophilized	Chitin-PLGA	Yes
Ding et al²	2.32 MPa to 2.17 MPa	No	Good	No	No	Coaxial spinning	Poly(L-lactic acid)/poly(lactide-co-glycolide) (PLLA/PLGA) core/shell	Yes
Vurat et al³	~20 kPa	No	Good	No	No	Microfluidic platform and bio printing	GelMA	No
Lee et al⁴	Not mentioned	Yes	Good	No	No	3D printing	Poly caprolactone /hydroxyapatite	Yes
Miranda et al⁵	Not mentioned	No	Good	No	No	Solution was frozen, and lyophilized	Chitosan-hyaluronic acid	No
Dubey et al⁶	~ 70kPa	No	Good	No	No	Melt electrowriting	Polycaprolactone	No
Staples et al⁷	Not mentioned	No	Good	No	yes	Melt electrowriting	Polycaprolactone	No

Table S2: Comparison table representing our proposed work and the other similar works

References:

- 1 S. Sowmya, U. Mony, P. Jayachandran, S. Reshma, R. A. Kumar, H. Arzate, S. V. Nair and R. Jayakumar, *Adv Healthc Mater*, 2017, **6**, 1–13.
- 2 T. Ding, J. Li, X. Zhang, L. Du, Y. Li, D. Li, B. Kong and S. Ge, *Biomater Sci*, 2020, **8**, 2459–2471.
- 3 M. T. Vurat, Ş. Şeker, Ö. Lalegül-Ülker, M. Parmaksiz, A. E. Elçin and Y. M. Elçin, *Genes Dis*, 2022, **9**, 1008–1023.
- 4 C. H. Lee, J. Hajibandeh, T. Suzuki, A. Fan, P. Shang and J. J. Mao, *Tissue Eng Part A*, 2014, **20**, 1342–1351.

- 5 D. G. Miranda, S. M. Malmonge, D. M. Campos, N. G. Attik, B. Grosgeat and K. Gritsch, *J Biomed Mater Res B Appl Biomater*, 2016, **104**, 1691–1702.
- 6 N. Dubey, J. A. Ferreira, A. Dagherery, Z. Aytac, J. Malda, S. B. Bhaduri and M. C. Bottino, *Acta Biomater*, 2020, **113**, 164–176.
- 7 R. J. Staples, S. Ivanovski and C. Vaquette, *J Periodontal Res*, 2020, **55**, 331–341.